PHYSICAL REVIEW B VOLUME 52, NUMBER 2 1 JULY 1995-II

Magnetic excitations in a highly frustrated pyrochlore antiferromagnet

M. J. Harris
ISIS Facility, Rutherford Appleton Laboratory, Chilton, Didcot, Oxon, OX11 0QX, United Kingdom

M. P. Zinkin
Oxford Physics, Clarendon Laboratory, Parks Road, Oxford, OX1 3PU, United Kingdom

T. Zeiske
Hahn-Meitner Institut, Glienickerstrasse 100, D-14109, Berlin, Germany

(Received 16 March 1995)

Spins that are coupled antiferromagnetically on the pyrochlore lattice are exposed to a high degree of geometrical frustration, resulting in the general absence of long-range order at all temperatures. We have investigated the inelastic response of the pyrochlore $CsNiCrF_6$ using neutron scattering. At positions where strong magnetic diffuse scattering has been observed we find a strong elastic signal, together with an unusual wing of inelastic scattering that is present even below the spin-glass transition of $CsNiCrF_6$. This indicates that while some of the magnetic fluctuations are being frozen out, others persist on a scale well in excess of the apparent spin-freezing temperature.

It is generally thought that instead of being a conventional long-range ordered structure, the ground state of the pyrochlore antiferromagnet is dynamically disordered at all temperatures down to 0 K, even though the exchange interactions may be very strong. This is because the magnetic ions sit at the corners of a network of corner-sharing tetrahedra (shown schematically in Fig. 1). The consequence is an extremely high degree of geometrical frustration because no possible spin configuration can satisfy all six antiferromagnetic interactions on a single tetrahedron. The pyrochlore lattice thus possesses much in common with the two-dimensional kagomé lattice and spin-$\frac{1}{2}$ triangular lattice antiferromagnets, which have been branded as possible "spin liquids." In terms of their geometry, the pyrochlore and kagomé lattices are the most strongly frustrated lattices possible.[1,2]

The problem of ordering on the pyrochlore lattice was considered nearly 40 years ago by Anderson,[3] who showed that long-range order may only exist if there are strong interactions on a length scale beyond the nearest neighbors. More recent mean-field and Monte Carlo calculations[1] support this view, which goes some way towards explaining the experimental observation that very few pyrochlore compounds appear to possess long-range magnetic order at any temperature. Those that do, such as FeF_3 (Refs. 4 and 5), and $Nd_2Mo_2O_7$ (Ref. 6) have noncoplanar magnetic structures characteristic of the strongly competing interactions present in the lattice.

In general, we expect that the infinite ground-state degeneracy of the pyrochlore lattice may be broken by a number of factors in addition to the effect of anomalously strong interactions beyond nearest neighbors, such as defects, and quantum and thermal fluctuations. These effects are present in every pyrochlore to some extent, although in the majority of cases they are evidently not strong enough to result in true long-range ordered structures. Instead, we may expect that a certain amount of short-range ordering will occur, which indeed appears to be the case in all of the pyrochlores that have been investigated experimentally.

This is the situation that occurs in the pyrochlore $CsNiCrF_6$, where no magnetic long-range order has been observed at any temperature, but single-crystal neutron-diffraction measurements[7] have shown that there is significant magnetic diffuse scattering. This indicates the presence of short-range order which is strongly antiferromagnetic and which only exists on the scale of nearest neighbors, even close to the spin-glass anomaly at about 2.3 K. This is a result of the intense frustration in the pyrochlore lattice. Note that the spin-glass transition temperature was measured carefully with a superconducting quantum interference device (SQUID) magnetometer.[8] It is now believed that the previously reported spin-glass temperature of 8 K in Ref. 7 was due to a spurious artifact of the previous experimental setup, since no significant anomaly was observed at this temperature in the SQUID experiment.

The most poorly understood, but potentially the most im-

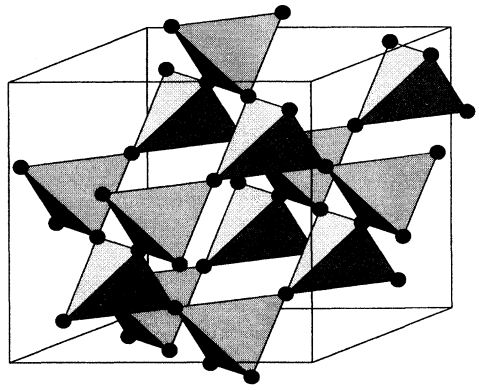

FIG. 1. The pyrochlore crystal structure with only the tetrahedral framework of the magnetic atoms shown.

portant aspect of such a highly frustrated system as a pyrochlore is its spin dynamics, since it is probably this that contains the real signature of the ground state, and reveals the extent to which its degeneracy is broken. This has become apparent from the extensive theoretical and experimental investigations that have been performed recently on the analogous problem of ordering on the kagomé lattice.[9,10] Our previous results for $CsNiCrF_6$ (Ref. 7) were obtained by measuring the static neutron-scattering cross section, $S(\mathbf{Q})$, by effectively integrating over all fluctuations within an energy window of about 4 meV. We have now extended these measurements to include the full inelastic response function. These results thus represent the determination of $S(\mathbf{Q},\omega)$ for a pyrochlore, and we observe many similarities with the behavior of the kagomé lattice compound $SrCr_8Ga_4O_{19}$.[10] In particular, we observe that the inelastic scattering is very broad in both wave vector, $\mathbf{Q}$, and energy, $\hbar\omega$, even below the spin-glass transition.

The measurements were performed using the PRISMA spectrometer at the ISIS spallation neutron facility (Rutherford Appleton Laboratory) and the E1 triple-axis spectrometer at the BER II reactor (Hahn-Meitner Institut). PRISMA is an indirect geometry time-of-flight spectrometer that is particularly well suited to measurements of weak and/or broad inelastic features, because a very large section of $(\mathbf{Q},\omega)$ space is accessible with a single setting of the instrument and a flat intrinsic background. Hence, we mainly used PRISMA to study the high temperature (above about 10 K) inelastic scattering from $CsNiCrF_6$, where the scattering is weaker and broader than at low temperatures.

A single crystal of $CsNiCrF_6$ with a volume of approximately 1 cm^3 was mounted with the [1 $\bar{1}$ 0] direction vertical, so that the scattering plane contained the reciprocal lattice vectors [4 4 0], [1 1 1], and [0 0 4]. Temperature control was achieved with a closed-cycle refrigerator on PRISMA, and a helium cryostat on E1. PRISMA was configured so that inelastic spectra were measured with eight analyzer-detector arms, each with an analyzing energy of 18 meV. This resulted in an energy resolution of 1.0 meV at the energy transfer $\hbar\omega=0$. On E1, we used an analyzing energy of 14 meV, which resulted in an energy resolution of 1.25 meV. Diffraction measurements were also performed simultaneously on PRISMA using eight additional detector arms that had no analyzer crystals. This allowed for a consistency check to compare with our earlier diffraction results,[7] while integrating the fluctuations over a much greater energy range (between 20 and 80 meV depending on the wave-vector transfer). We found no significant differences with our earlier measurements, indicating that the majority of the fluctuations are less than about 4 meV in extent.

Single-crystal neutron-diffraction work[7] has shown that the magnetic diffuse scattering is strongest along the [1 1 0] zone of reciprocal space in $CsNiCrF_6$, with maxima at the (1.5 1.5 0) and (2.5 2.5 0) positions (where $Q=1.3$ and 2.2 $Å^{-1}$, respectively). With PRISMA, we performed inelastic scans through the diffuse maximum at (2.5 2.5 0) with sample temperatures of 8.3, 15, 20, 30, 50, 100, and 150 K. Even though the scattering is weaker here than at the (1.5 1.5 0) position, we found that we achieved a better signal-to-noise ratio. This is because the spectrometer configuration required for the (1.5 1.5 0) position is less favorable, and results in a high background. Hence, we concentrated on the (2.5 2.5 0) position in our PRISMA measurements, although a number of scans were performed at other positions in reciprocal space. These scans are not strictly constant-Q scans as one would perform on a triple-axis spectrometer, but instead are parabolic cuts through $(\mathbf{Q},\omega)$ space. Thus, for the scans through the (2.5 2.5 0) position, the wave-vector transfer ranges from $\mathbf{Q}=(2.7\ 2.7\ \bar{1})$ when the energy transfer is $\hbar\omega=-5$ meV, to $\mathbf{Q}=(2.2\ 2.2\ 1.5)$ when $\hbar\omega=10$ meV, so that they cut through the maximum of the magnetic diffuse scattering at $\mathbf{Q}=(2.5\ 2.5\ 0)$ when $\hbar\omega=0$. On E1, we performed straightforward constant-Q scans at (2.5 2.5 0) and a number of other positions, at sample temperatures of 1.6, 4, 9, and 69 K.

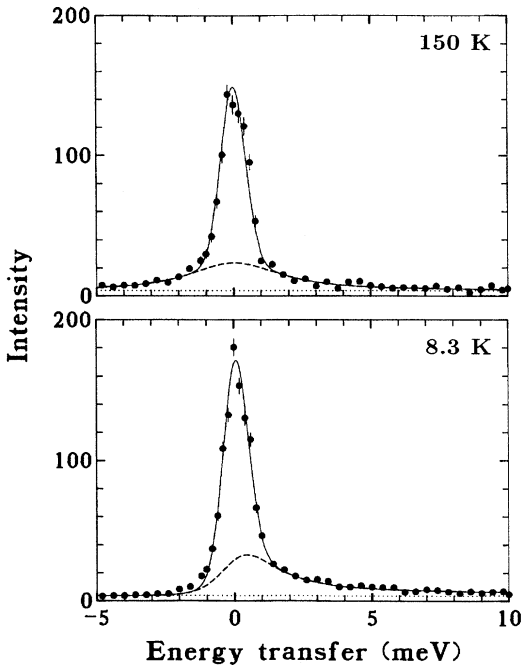

FIG. 2. Inelastic spectra at the (2.5 2.5 0) position, measured on PRISMA at sample temperatures of 8.3 and 150 K. The solid curves show the results of fits to the full scattering cross section discussed in the text, while the broken lines show the magnetic contribution, which clearly sharpens as the temperature is lowered. The dotted lines show the background in each case. The intensity scale is in abitrary units.

In Fig. 2 we show the results of the PRISMA scans through the (2.5 2.5 0) position for the lowest and highest sample temperatures measured on PRISMA, which are 8.3 and 150 K, respectively. Although data were collected over the range -12 to 50 meV in energy transfer, only the reduced range of -5 to 10 meV is shown in the figure, in order to emphasize the scattering around $\hbar\omega=0$. There is a strong nuclear incoherent component to the scattering, and as the sample is cooled the magnetic signal develops as a strong elastic component with a wing extending to higher energies. Similar results were found at other positions of maximum diffuse scattering such as (1.5 1.5 0) and (0.5 0.5 2), while at the minimum around (2 2 2) we observed only the nuclear

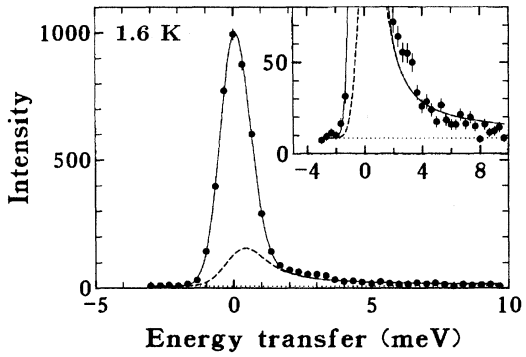

FIG. 3. The inelastic scattering at the (2.5 2.5 0) position, measured at a sample temperature of 1.6 K with the triple-axis spectrometer E1. The solid curve shows a fit to the full scattering cross section, while the broken line shows the magnetic contribution, and the dotted line shows the background. In the inset, we show the data on an expanded scale to emphasize the inelastic wing extending to high energies. The intensity scale is in counts per monitor (approximately 15 min).

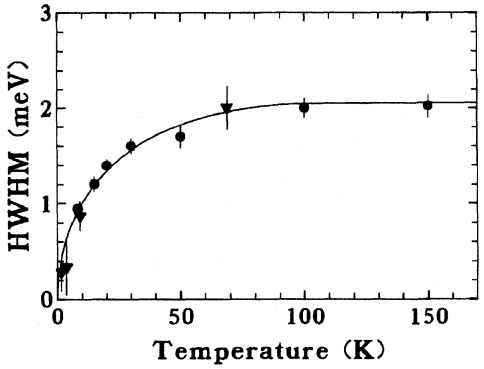

FIG. 4. The half-width (HWHM) of the magnetic component of the scattering. The curve is a guide to the eye, and extrapolates to 0 meV at 0 K. The PRISMA results are shown by the circles, and the E1 results by the triangles.

incoherent scattering, which is characterized simply by a δ function at $\hbar\omega=0$. In Fig. 3 we show the scattering measured at the (2.5 2.5 0) position with a sample temperature of 1.6 K on E1. The wing of inelastic scattering is still present even at this low temperature.

We used the following scattering cross section in the data analysis:

$$\frac{\partial^2\sigma}{\partial\Omega\,\partial\omega}=A\,\frac{k_f}{k_i}\,\frac{\hbar\omega/k_BT}{1-\exp(-\hbar\omega/k_BT)}|f(\mathbf{Q})|^2\chi_0\chi(\mathbf{Q})F(\mathbf{Q},\omega)+B(T)\,\delta(\omega), \quad (1)$$

where the first term represents the magnetic scattering, and the second represents the nuclear incoherent scattering. A and B are proportionality coefficients (B is slightly temperature dependent), k_i and k_f are the magnitudes of the wave vectors of the incident and scattered neutrons, respectively, $f(\mathbf{Q})$ is the magnetic form factor, χ_0 is the single-ion susceptibility, and $\chi(\mathbf{Q})$ is the static susceptibility. Since $\mathbf{Q}$ varies in a PRISMA scan, it is necessary to know the product $|f(\mathbf{Q})|^2\chi_0\chi(\mathbf{Q})$, and this was obtained directly from the diffraction scans measured at every temperature, which covered the required $\mathbf{Q}$ trajectory. The inelastic response function $F(\mathbf{Q},\omega)$ represents spin diffusion in an exchange-coupled paramagnet:[11]

$$F(\mathbf{Q},\omega)=\frac{\Gamma}{\pi}\,\frac{1}{\Gamma^2+\omega^2}\,. \quad (2)$$

Thus, the inelastic data were analyzed by least-squares fitting with two components: a Gaussian peak centered on zero energy to represent the nuclear incoherent scattering, and a Lorentzian peak, also centered on zero energy, to represent the magnetic scattering. The nuclear component represents the experimental resolution function, and its width was kept fixed at the resolution width. Its amplitude varies slightly with temperature due to the effect of the Debye-Waller factor, however, and the relative dependence was determined from the behavior of the nuclear Bragg peaks.

In Figs. 2 and 3 we show the fits of Eq. (1) to the experimental data as solid curves, with the magnetic part as dashed lines. Note that although the magnetic component is actually centered on $\hbar\omega=0$, it appears to be offset by approximately 0.5 meV in the 8.3 K data in Fig. 2, and in Fig. 3. This is simply due to the effect of the resolution convolution on the detailed balance factor, which has a sharp step at $\hbar\omega=0$ for low temperatures. The agreement is good for all of the data collected with sample temperatures of 8.3 K and above. However, the quality of fit is significantly poorer for the 1.6 and 4 K data, as is apparent in the inset to Fig. 3. Below the spin-freezing temperature, the simple model of spin diffusion (which represents a single relaxational process) is no longer appropriate to describe the spin dynamics. A better model would include a higher density of excitations in the 2–10 meV range than does a Lorentzian. Very similar inelastic scattering has been observed in the analogous kagomé lattice system $SrCr_8Ga_4O_{19}$.[10]

The general behavior of the magnetic scattering is such that it becomes sharper as the temperature is lowered, signaling a general slowing down of the spin dynamics, and in Fig. 4, we show the behavior of the half-width at half maximum (HWHM) of the magnetic component with temperature for both the PRISMA and the E1 data. The half-width clearly decreases rapidly as the temperature is lowered below about 50 K. A similar result was found for the pyrochlore $Tb_2Mo_2O_7$, and the width of the magnetic scattering was observed to decrease below the resolution limit at the 25 K spin-glass anomaly.[12] However, no wing of inelastic scattering was observed in $Tb_2Mo_2O_7$ extending beyond the energy equivalent of the spin-freezing temperature, as is observed in $CsNiCrF_6$. We note in passing that the Q dependence of the width of the magnetic scattering in $CsNiCrF_6$ is consistent with the diffusion law $\Gamma\propto Q^2$.

What is remarkable about $CsNiCrF_6$ is that even in the scans measured at 1.6 K (which converts to an energy of $k_BT=0.14$ meV), there is still significant inelastic intensity extending out to at least 7 meV; this energy is more than an order of magnitude greater than k_BT. The sample temperature of 1.6 K is well below the apparent spin-glass temperature of 2.3 K, and we would then normally expect there to be no inelastic processes greater than about k_BT. Hence, our

observation of an inelastic wing in addition to the usual elastic scattering implies that while some of the spin fluctuations are being frozen out, there are others existing on a scale well in excess of these. This highly unusual behavior shows that although $CsNiCrF_6$ possesses what looks like a conventional spin-glass anomaly in the susceptibility, its spin dynamics show it to be very different from a classic spin glass. A similar observation was made for $SrCr_8Ga_4O_{19}$.[10]

This type of behavior is reminiscent of a soft mode at a structural phase transition, where a spontaneous structural change is driven by the freezing out of a particular phonon mode. Like Broholm *et al.*,[10] we speculate that we are observing the appearance of a novel type of magnetic order that is not directly observable in the usual way, through the appearance of magnetic Bragg peaks, for instance. This is because the order is not strictly static, but has a significant dynamic component. In ac-susceptibility or magnetization experiments (which are sensitive to fluctuations on a much slower time scale than neutron scattering) it is manifest as a cusp, similar to a conventional spin-glass anomaly.

The financial support of the EPSRC is gratefully acknowledged. We thank R. A. Cowley, M. Steiner, and U. Steigenberger for helpful discussions.

[1] J. N. Reimers, A. J. Berlinsky, and A. C. Shi, Phys. Rev. B **43**, 865 (1991); J. N. Reimers, Phys. Rev. B **45**, 7287 (1992).

[2] P. Lacorre, J. Phys. C **20**, L775 (1987).

[3] P. W. Anderson, Phys. Rev. **102**, 1008 (1956).

[4] G. Ferey, R. de Pape, M. Leblanc, and J. Pannetier, Rev. Chim. Miner. **23**, 474 (1986).

[5] J. N. Reimers, J. A. Greedan, and M Björgvinsson, Phys. Rev. B **45**, 7295 (1992).

[6] J. E. Greedan, J. N. Reimers, C. V. Stager, and S. L. Penny, Phys. Rev. B **43**, 5682 (1991).

[7] M. J. Harris, M. P. Zinkin, Z. Tun, B. M. Wanklyn, and I. P. Swanson, Phys. Rev. Lett. **73**, 189 (1994).

[8] M. P. Zinkin, M. J. Harris, and S. Carling (unpublished).

[9] J. T. Chalker, P. C. W. Holdsworth, and E. F. Shender, Phys. Rev. Lett. **68**, 855 (1992); A. B. Harris, C. Kallin, and A. J. Berlinsky, Phys. Rev. B **45**, 2899 (1992); A. Chubukov, Phys. Rev. Lett. **69**, 832 (1992); A. Keren, *ibid.* **72**, 3254 (1994).

[10] C. Broholm, G. Aeppli, G. P. Espinosa, and A. S. Cooper, Phys. Rev. Lett. **65**, 3173 (1990).

[11] S. W. Lovesey, *Theory of Neutron Scattering from Condensed Matter* (Clarendon, Oxford, 1984), Vol. 2.

[12] B. D. Gaulin, J. N. Reimers, T. E. Mason, J. E. Greedan, and Z. Tun, Phys. Rev. Lett. **69**, 3244 (1992).

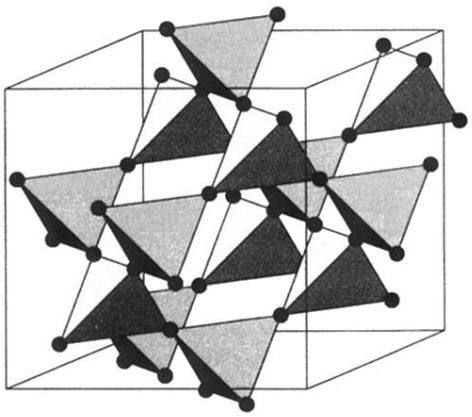

FIG. 1. The pyrochlore crystal structure with only the tetrahedral framework of the magnetic atoms shown.